

A CRITICAL ANALYSIS OF PROPOSED POWER LOMAX GEOMETRIC DISTRIBUTION

Muhammad Saqib^{1§}, Ahmed Zogo Memon² and Sohail Chand³

College of Statistical and Actuarial Sciences,
University of the Punjab, Lahore, Pakistan

Email: ¹ saqibp0516@gmail.com

² azogo.memon@gmail.com

³ sohail.stat@pu.edu.pk

ORCID ID: ¹ <https://orcid.org/0000-0003-3831-8404>

² <https://orcid.org/0000-0001-6171-0186>

³ <https://orcid.org/0000-0002-4564-143X>

§ Corresponding author

ABSTRACT

The probability model ‘Power Lomax Geometric Distribution’ proposed in this paper is derived from Power Lomax distribution through its compounding with the Geometric distribution. We present its various theoretical properties including hazard function, mean residual life and entropy. The family of this distribution constitutes heterogeneous characteristics, and is so classified into three distinguishable subfamilies. Each subfamily is unique in its importance with respect to theoretical and practical applications. The ML method is used for the estimation of four parameters of this distribution. To assess its adequacy we consider four real life data sets comparing it with other fitted models in literature. The model is flexible in its applicability to a large number of different situations.

KEYWORDS

Characterization, hazard function, mean residual life, Shannon entropy.

1. INTRODUCTION

Various probabilistic models are available in statistical literature for their description of datasets relating to industrial, medical and other sciences. Lomax (1954) introduced a two parameter distribution for modeling life datasets in industry and later it was widely used in other scientific fields. As for a few references, Harris (1968) studied the income and wealth data through the application of Lomax distribution. Bryson (1974) suggested it as an alternative to the exponential distribution when the dataset is heavy-tailed. Atkinson and Harrison (1979) applied Lomax model in modeling business failure data. The distribution also has its applications in modeling the sizes of computer files on servers Holland et al. (2006). Corbellini et al. (2010), Amal S. Hassan & Al-Ghamdi (2009) etc. are some other papers which focus on Lomax distribution for its reliability studies and life testing. A number of extensions of the Lomax model have been developed by various authors. Some of these distributions are for instance Marshall–Olkin extended-Lomax (Ghitany et al., 2007), Extended-Lomax (Lemonte & Cordeiro, 2013), Gamma-Lomax

(Cordeiro et al., 2015), Exponentiated Lomax Geometric distributions (Amal Soliman Hassan & Abd-Allah, 2017). The compounding of probability distributions has also been a useful approach in producing flexible models. Some of these models, for instance, are Exponential-geometric distribution by Adamidis & Loukas (1998), Generalized linear Exponential Geometric distribution by Okasha & Al-Shomrani (2019) and the Quasi Xgamma Geometric distribution by Sen et al. (2019) etc. These generalized models have their specific applications in scientific fields but there are situations where the existing models in literature fail to fit adequately.

Rady et al. (2016) proposed Power Lomax distribution (POLOD) with pdf

$$f(x) = \alpha\beta\lambda^\alpha x^{\beta-1} (\lambda + x^\beta)^{-(\alpha+1)}, \quad x > 0 \quad (1)$$

providing its applications where $\alpha > 0, \beta > 0$ and $\lambda > 0$ are parameters. In this paper, we develop Power Lomax Geometric Distribution (POLOGD) through mixing of Power Lomax distribution with Geometric distribution through an additional parameter. We study its various theoretical properties assessing the role of this parameter and provide its applications.

The material organized in this paper is as follows. In Section 2, the proposed POLOGD is derived and its special cases are discussed. In Section 3, we state and prove a theorem on characterization of this distribution. Section 4 considers three subfamilies of POLOGD distributions that are heterogeneous with respect to the shapes of their density curves. Its quantile function, moments, skewness, kurtosis, hazard and mean residual life (MRL) etc are obtained in Section 5. A comparison is made POLOGD versus POLOD in Section 6. Finally, the ML estimates of distribution's parameters are studied through simulation procedure in Section 7. Its applications to published datasets are also given in this section. Proofs of some mathematical theorems in this paper are included in the Appendix.

2. FORMULATION OF MODEL

Let x_1, x_2, \dots, x_N be a random sample of size N from POLOD with pdf as defined in Eq. (1). Suppose that N is a zero-truncated geometric random variable with pmf $f(n) = (1-p)p^{n-1}; n = 1, 2, \dots, \infty, p \in (0, 1)$. If $X_{(1)} = \min\{X_1, X_2, \dots, X_N\}$ is the first order statistic its conditional pdf given $N = n$ is $f_1(x|n) = n\alpha\beta\lambda^\alpha x^{\beta-1} \left(\lambda^\alpha (\lambda + x^\beta)^{-\alpha} \right)^{n-1} (\lambda + x^\beta)^{-(\alpha+1)}$. From the joint distribution of (X, N) , it can be seen that the probability density function of X simplifies to

$$f(x; \phi) = \frac{(1-p)\alpha\beta\lambda^\alpha x^{\beta-1} (\lambda + x^\beta)^{-(\alpha+1)}}{\left(1 - p\lambda^\alpha (\lambda + x^\beta)^{-\alpha} \right)^2}, \quad x > 0 \quad (2)$$

where $\phi = \{\alpha, \beta, \lambda, p\}$ is the set of parameters with $\alpha, \beta, \lambda > 0$ and $p \in (0, 1)$. Defining it as the pdf of POLOGD random variable X , we obtain its cumulative distribution function (cdf)

$$F(x; \phi) = \frac{\left(1 - \lambda^\alpha (\lambda + x^\beta)^{-\alpha}\right)}{\left(1 - p\lambda^\alpha (\lambda + x^\beta)^{-\alpha}\right)}, \quad x > 0 \quad (3)$$

2.1 Special Cases

Burr-XII Geometric (B-XIIG) distribution (Korkmaz & Erisoglu, 2014) follows from the proposed POLOGD for $\lambda = 1$. However, as p approaches zero we obtain the Power Lomax distribution (POLOD) (Rady et al., 2016), Lomax distribution (LOD) (Lomax, 1954) for $\beta = 1$, Burr-XII (B-XII) distribution (Burr, 1942) for $\lambda = 1$.

3. CHARACTERIZATION OF POLOGD

We use the well-known theorem by Glänzel (1987) for the characterization of a distribution where $q_1(X)$ and $q_2(X)$ are real functions of the random variable X such that

$$E(q_2(X) | X > x) = E(q_1(X) | X > x)\eta(x)$$

where $\eta(x)$ is real function of x . If $\eta q_1 = q_2$ has no real solution then the cdf of X can be uniquely determined by the functions q_1, q_2 and η . In the context of this theorem, we determine the functions $q_1(X)$ and $q_2(X)$ with reference to POLOGD.

Theorem 1

The functions $q_1(X)$ and $q_2(X)$ relating to POLOGD for its characterization under Glänzel's theorem are

$$q_1(X) = \left(1 - p(1 + X^\beta \lambda^{-1})^{-\alpha}\right)^2$$

$$q_2(X) = q_1(X)(1 + X^\beta \lambda^{-1})^{-\alpha}.$$

Proof:

By using the pdf and cdf of POLOGD, it can be shown that the conditional expectations of the functions $q_1(X)$ and $q_2(X)$ are

$$E(q_1(X) | X > x) = \lambda(1-p)(1-F(x))^{-1}(1+x^\beta \lambda^{-1})^{-\alpha}, \quad x > 0$$

and

$$E(q_2(X) | X > x) = \frac{1}{2}\lambda(1-p)(1-F(x))^{-1}(1+x^\beta \lambda^{-1})^{-2\alpha}, \quad x > 0.$$

So that the ratio $E(q_2(X)|X>x)/E(q_1(X)|X>x)$ simplifies to $\eta(x)=\frac{1}{2}\left(1+x^\beta\lambda^{-1}\right)^{-\alpha}$.

Also

$$\eta(x)q_1(x)-q_2(x)=-\frac{1}{2}\left(1+\frac{x^\beta}{\lambda}\right)^{-\alpha} q_1(x) \quad \neq 0, x > 0.$$

Conversely, with $\eta(x)$ as the above expression we have

$$s'(x)=\frac{\eta'(x)q_1(X)}{\eta(x)q_1(X)-q_2(X)}=\frac{\alpha\beta}{\lambda}x^{\beta-1}\left(1+\frac{x^\beta}{\lambda}\right)^{-1}, \quad x > 0$$

and so

$$s(x)=\ln\left(1+\frac{x^\beta}{\lambda}\right)^\alpha, \quad x > 0$$

and the expression

$$F(x)=\int_a^x C \left| \frac{\eta'(x)}{\eta(x)q_1(x)-q_2(x)} \right| e^{-s(x)} dx$$

where C is a normalizing constant and $a=0$ in this case

$$= \frac{\alpha\beta(1-p)}{\lambda} \int_a^x x^{\beta-1} \left(1+\frac{x^\beta}{\lambda}\right)^{-\alpha-1} \left(1-p\left(1+\frac{x^\beta}{\lambda}\right)^{-\alpha}\right)^{-2} dx$$

which ultimately simplifies to the cdf of POLOGD.

3.1 Corollary

On substituting the relevant values of POLOGD parameters in the Theorem 1 we can now characterize the distributions mentioned above under the special cases.

4. SUBFAMILIES OF POLOG DISTRIBUTION

The pdf curves of POLOG distributions have different heterogeneous shapes. We explore here parametric restrictions to generate subfamilies of POLOGD that display similarity of shapes of the pdf curves of the members within each subfamily.

The limit of POLOG pdf $f(x)$ as $x \rightarrow 0$ is

$$\lim_{x \rightarrow 0} f(x) = \lim_{x \rightarrow 0} \frac{(1-p)\alpha\beta\lambda^\alpha x^{\beta-1} (\lambda+x^\beta)^{-(\alpha+1)}}{\left(1-p\lambda^\alpha (\lambda+x^\beta)^{-\alpha}\right)^2} = \begin{cases} \infty & , \beta < 1 \\ \alpha & , \beta = 1. \\ 0 & , \beta > 1 \end{cases} \quad (4)$$

With $\lim_{x \rightarrow \infty} f(x) = 0$ it follows that parameter β plays a conspicuous role in differentiating the shapes of POLOG density curves. That is, the family of POLOG distributions broadly disintegrates into the following three subfamilies.

$$\begin{cases} \text{Subfamily-1} & x : \beta < 1; \alpha; \lambda > 0; p \in (0,1) \\ \text{Subfamily-2} & x : \beta = 1; \alpha; \lambda > 0; p \in (0,1) \\ \text{Subfamily-3} & x : \beta > 1; \alpha; \lambda > 0; p \in (0,1). \end{cases}$$

4.1 Trends of POLOG pdf Curves at $x = 0$

At the origin the pdf curves of the members of the first subfamily begin with a downward trend whereas the density curves of the distributions in the third subfamily move upward. For the second subfamily with $\beta = 1$ the density curves of the distributions trend below the limit $\alpha/\lambda(1-p)$ on the vertical axis at $x = 0$. It is easy to verify that the density function $f(x)$ of the first and second POLOGD subfamilies assumes a decreasing value as x increases.

The following graphs illustrate the pdf curves of some members of the POLOGD subfamilies for varying value of the parameter p .

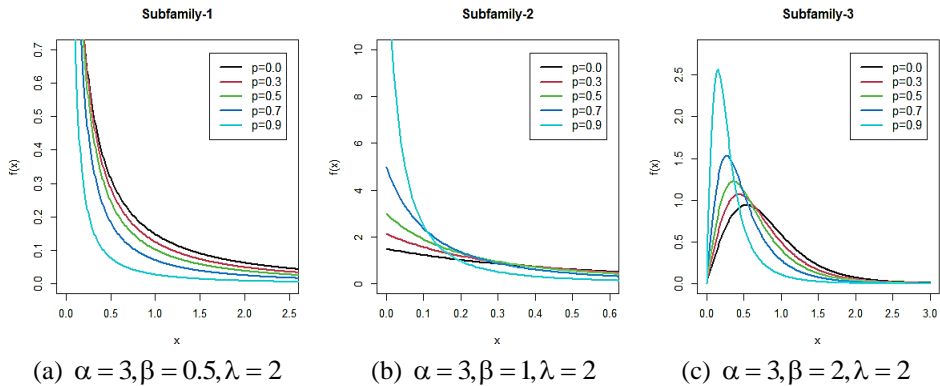


Figure 1: pdf Curves of POLOGD with $\beta < 1$, $\beta = 1$ and $\beta > 1$

From Figure 1 it can be observed that with the increasing value of p along the tails of $f(x)$ become narrow and its mode shifts to the left. The density curves in the first subfamily remain L-shaped. The height $\alpha/\lambda(1-p)$ of $f(x)$ at $x = 0$ increases in the second subfamily. The pdf curves in the third subfamily begin at $x = 0$ assuming different shapes with longer tails for larger p values.

5. CHARACTERISTICS OF POLOGD

We discuss below some important properties of the proposed distribution.

5.1 Quantiles

The q th quantile x_q of the distribution follows from $F[x_q; \phi] = q$ and is given as

$$x_q = \lambda^{\frac{1}{\beta}} \left[\left\{ \frac{(1-qp)}{(1-q)} \right\}^{\frac{1}{\alpha}} - 1 \right]^{\frac{1}{\beta}}. \quad (5)$$

Assuming that a particular parameter changes and its other three parameters remain fixed, it is found that the quantile x_q

- i) Decreases if α or p increases.
- ii) Increases if λ increases.

iii) a) Increases if β increases and $\left((1-qp)(1-q)^{-1} \right) < (1+\lambda^{-1})^\alpha$.

b) Decreases if β increases and $\left((1-qp)(1-q)^{-1} \right) > (1+\lambda^{-1})^\alpha$.

The proofs of above assertions are briefly presented in Appendix A1.

In particular the median following from above simplifies to

$$x_{0.5} = \lambda^{\frac{1}{\beta}} \left[(2-p)^{\frac{1}{\alpha}} - 1 \right]^{\frac{1}{\beta}}. \quad (6)$$

It is easy to see that the median of POLOG distributions occurs at $x=1$ for $p=1/2$ and $2(1+\lambda^{-1})^\alpha = 3$. Thus for different values of the parameters α and λ , there exist a large number of POLOG distributions with the same median 1.

5.2 Mode

From Eq. (4), it is clear that the mode of Subfamily 1 does not exist. For the second subfamily as discussed in Section 4, it has mode at $x=0$. The mode of a distribution in the third subfamily is determined by the solution of the equation $f'(x)=0$, that is,

$$(\beta-1)(\lambda+x^\beta) = \beta x^\beta \left[(\alpha+1) + 2\alpha p \left((\lambda+x^\beta)^\alpha - p\lambda^\alpha \right)^{-1} \right]. \quad (7)$$

The modes of some selected distributions of Subfamily 3 are given Table 5 in Appendix A2. The mode of a distribution in this subfamily increases as the values of β or λ increase; and decreases as α or p increases.

5.3 Moments of POLOGD

The r th moment of a POLOG distribution is

$$\mu'_r = (1-p)\alpha\beta\lambda^\alpha \int_0^\infty x^{r+\beta-1} (\lambda+x^\beta)^{-(\alpha+1)} \left(1-p\lambda^\alpha (\lambda+x^\beta)^{-\alpha}\right)^{-2} dx.$$

On using the expansion

$$(1-z)^{-k} = \sum_{j=0}^\infty \binom{k+j-1}{k-1} z^j, \quad |z| < 1, k > 0$$

the above reduces to

$$(1-p)\alpha\beta \sum_{j=0}^\infty w_j \lambda^{\alpha(j+1)-\alpha(j+1)-1} \int_0^\infty x^{r+\beta-1} \left(1+\frac{x^\beta}{\lambda}\right)^{-\alpha(j+1)-1} dx$$

where $w_j = (j+1)p^j$.

Let $t = \frac{x^\beta}{\lambda}$. Under this transformation, the r th moment in terms of Beta functions are given as

$$\begin{aligned} \mu'_r &= \alpha(1-p) \sum_{j=0}^\infty w_j \lambda^{\frac{r}{\beta}} \int_0^\infty t^{\frac{r}{\beta}+1-1} \frac{1}{(1+t)^{\alpha(j+1)-\frac{r}{\beta}+\frac{r}{\beta}+1}} dt \\ &= \alpha(1-p) \sum_{j=0}^\infty w_j \lambda^{\frac{r}{\beta}} B\left(\frac{r}{\beta}+1, \alpha(j+1)-\frac{r}{\beta}\right) \end{aligned} \tag{8}$$

provided the condition $\alpha\beta > r$ holds.

It follows that the mean of a POLOG distribution with $\alpha\beta > 1$ is

$$\mu'_1 = \alpha(1-p)\lambda^{\frac{1}{\beta}} \sum_{j=0}^\infty (j+1)p^j B\left(\frac{1}{\beta}+1, \alpha(j+1)-\frac{1}{\beta}\right) \tag{9}$$

As the quantity $(p^j - p^{j+1})$ decreases with increasing p , it follows that for other parameters fixed μ'_1 decreases as p increases. Also, as $p \rightarrow 0$, it simplifies to the mean $\alpha\lambda^{\frac{1}{\beta}} B\left(\frac{1}{\beta}+1, \alpha-\frac{1}{\beta}\right)$ of POLOG in (Rady et al., 2016). That is, the mean of a POLOG distribution with fixed α, β and λ serves as the upper bound of the mean of POLOG distribution.

As for the effects of other parameters, we can use Table 5 in Appendix A2 that shows the means of several POLOG distributions. Based on it we observe that the mean of POLOGD in each subfamily increases when λ or β increases while the other two parameters remain fixed. On the contrary the mean decreases by increasing α .

5.4 Skewness and Kurtosis

The family of POLOG distributions has a wide variation in its shapes depending primarily on the parameter β . We discuss here the skewness and kurtosis aspects of these distributions.

The r th moment about mean of POLOG distribution is obtained through the relation $\mu_r = \sum_{k=0}^r \binom{r}{k} (-1)^k \mu'_{r-k} (\mu')^k$. By using the relevant moments, we additionally determine the coefficients of skewness and kurtosis of the distributions.

Based on Table 5 in Appendix A2, we discover that the coefficient of skewness of a distribution in Subfamily 1 diminishes when β increases or p decreases. The distributions in Subfamily 2 with $\beta = 1$ display longer positively skewed tails when p increases. In Subfamily 3 the coefficient first decreases and then increases depending on the value of β and p . Some of the distributions in this subfamily are nearly symmetrical. As for the increase in α , the coefficient of skewness decreases for all subfamilies.

With regard to kurtosis, we observe more or less a pattern similar to that of skewness when the parameters vary.

5.5 Hazard Function

The hazard function of POLOGD is

$$h(x) = \frac{\alpha \beta x^{\beta-1} (\lambda + x^\beta)^{\alpha-1}}{(\lambda + x^\beta)^\alpha - p \lambda^\alpha}, \quad x > 0. \quad (10)$$

It is easy to observe that

$$\lim_{x \rightarrow 0} h(x) = \begin{cases} \infty & \beta < 1 \\ \frac{\alpha}{\lambda(1-p)} & \beta = 1 \\ 0 & \beta > 1 \end{cases}$$

and $\lim_{x \rightarrow \infty} h(x) = 0$.

From above it follows that the hazard curves of POLOG distributions do not show similarity in their shapes.

Remarks:

The hazard function of POLOGD has the following properties.

- i) The shape of a hazard curve of the distribution is primarily dependent on β . Let us first assume that this parameter varies and the other parameters are fixed, the expression (10) for $h(x)$ and the function $\alpha \beta x^{\beta-1} / (\lambda + x^\beta)$ are expected to display similar shapes of their curves. To have a general idea about the shape of POLOGD hazard

curves, we can consider the shape aspects of function $g(x)$ defined in Appendix A3 and conclude to have the following a general idea that the shape of POLOGD hazard curves:

- a. Decreases with increasing value of x in its first and second subfamilies.
- b. Describes a downward bathtub for the distributions in the third subfamily.

The critical point x_0 of a POLOGD hazard curve in the third subfamily is determined from a complicated equation $h'(x) = 0$. In Figure 2 for illustration, we provide the hazard curves relating to POLOGD subfamilies with parametric values as follows:

- a. $0 < \beta \leq 1, \alpha = 3, \lambda = 2, p = 0.5$. The hazard curves based on $\beta = \{0.1, 0.3, 0.5, 0.7, 1\}$.
- b. $\beta > 1, \alpha = 3, \lambda = 2, p = 0.5$. The hazard rates relating to $\beta = \{2, 3, 5, 7\}$.

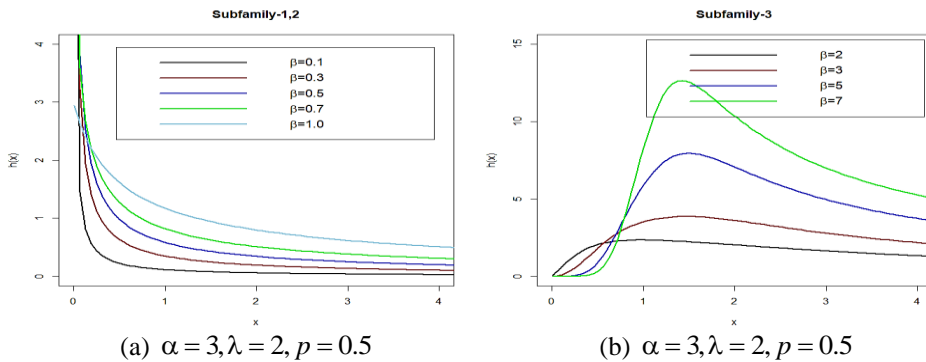


Figure 2: Hazard Curves of POLOGD for $\beta \leq 1$ and $\beta > 1$

As for the significance of other shape parameters in the POLOGD hazard function, we state and prove the following theorems displaying the effect of varying a parameter when the other three parameters are fixed.

ii) The hazard function of POLOGD increases when its parameter p alone increases.

For proof, let $p_1 < p_2$ and the other parameters remain fixed. Then, since

$$-p_1\lambda^\alpha > -p_2\lambda^\alpha$$

$$(\lambda + x^\beta)^\alpha - p_1\lambda^\alpha > (\lambda + x^\beta)^\alpha - p_2\lambda^\alpha$$

taking reciprocal the above simplifies to

$$\frac{\alpha\beta x^{\beta-1}(\lambda + x^\beta)^{\alpha-1}}{(\lambda + x^\beta)^\alpha - p_1\lambda^\alpha} < \frac{\alpha\beta x^{\beta-1}(\lambda + x^\beta)^{\alpha-1}}{(\lambda + x^\beta)^\alpha - p_2\lambda^\alpha}$$

and the result follows.

The following graphs illustrate the above property.

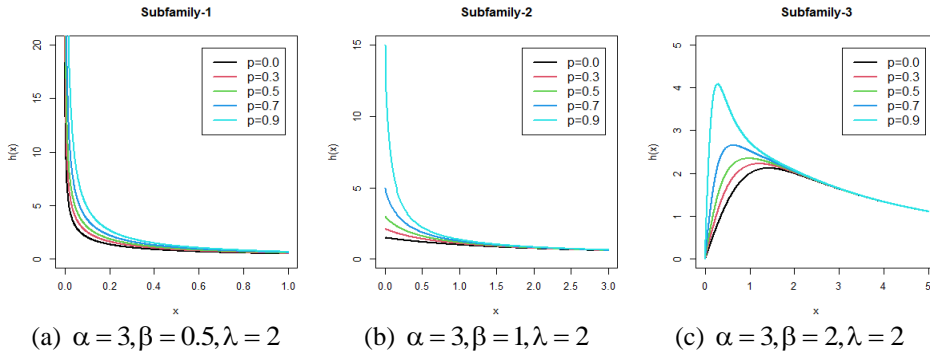


Figure 3: Hazard Curves of POLOGD for different p Values when $\beta < 1$, $\beta = 1$ and $\beta > 1$

POLOGD being a generalization of POLOGD has an additional parameter p . As this parameter varies a new distribution appears with its hazard property different from that of POLOGD thus enhancing its versatility for applications. We conclude from the above mathematical result that:

- a. A larger p value in the POLOGD model causes a larger hazard rate causing the risk for a shorter life of the product. It follows that the life of a product under the POLOGD model takes a longer time for its expiry when compared with the product based on a POLOGD model.
- b. The lower bound of a POLOGD hazard rate is $\alpha\beta x^{\beta-1} / (\lambda + x^\beta)$, which is the hazard rate of POLOGD.

iii) The hazard function of POLOGD increases when α increases.

For its proof, we write hazard function in the form

$$\alpha\beta x^{\beta-1} / (\lambda + x^\beta) \left(1 - p \left(\lambda / (\lambda + x^\beta) \right)^\alpha \right).$$

For fixed x, β, λ, p and varying α , we can

prove the result by applying Lemma 1 (see Appendix A4) with $c = (\lambda / (\lambda + x^\beta)) < 1$.

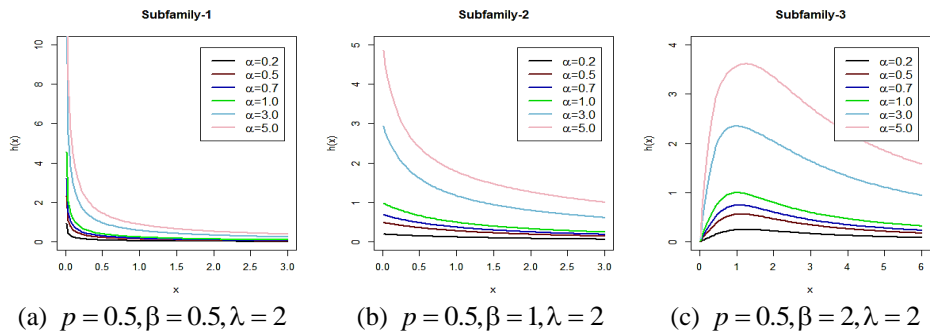


Figure 4: Hazard Curves of POLOGD for Different α Values when $\beta < 1$, $\beta = 1$ and $\beta > 1$

5.6 Mean Residual Life of POLOGD

On using a similar approach as in Section 5.3, it can be shown that the mean residual life of the distribution simplifies to

$$\frac{1}{\beta} \left[\left(1 + \frac{x^\beta}{\lambda} \right)^\alpha - p \right] \sum_{j=0}^{\infty} p^j B \left[\frac{x^\beta}{\lambda}, \frac{1}{\beta}, \alpha(j+1) - \frac{1}{\beta} \right] \quad \text{for } \alpha\beta > 1. \quad (11)$$

The graphs of MRL curves are presented below for the same members of POLOGD subfamilies as in Figure 3.

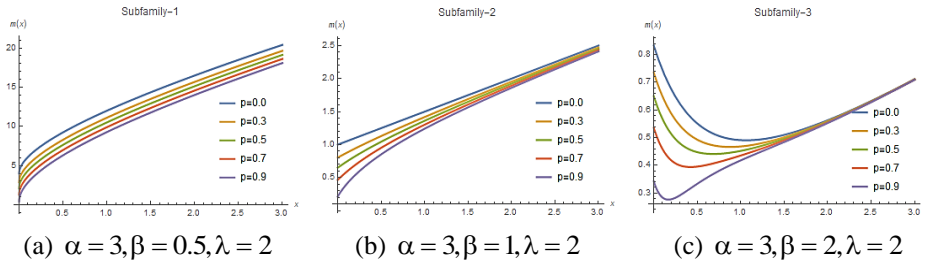


Figure 5: MRL of a POLOGD for different p values when $\beta < 1$, $\beta = 1$ and $\beta > 1$

As follows from the above graphs the MRL decreases with the increasing value of p in each subfamily. The behavior of these graphs is opposite to that of the hazard curves in Figure 3. The MRL of a POLOG distribution with fixed parameters α, β and λ does not exceed a value mentioned in the following corollary.

5.7 Corollary

- i) As $p \rightarrow 0$, the MRL for POLOGD simplifies to $\frac{1}{\beta} \left(1 + \frac{x^\beta}{\lambda} \right)^\alpha B \left[\frac{x^\beta}{\lambda}, \frac{1}{\beta}, \alpha - \frac{1}{\beta} \right]$ for $\alpha\beta > 1$ as in (Rady et al., 2016).
- ii) It is easy to prove that the MRL of POLOGD assumes a decreasing trend as p alone increases towards its upper bound that is the MRL of POLOG.

6. POLOGD VERSUS POLOG

The generalization of POLOGD through the additional parameter p has produced useful distributions to cover additional datasets for fitting. We find in our above study that this parameter plays an important role in heterogeneous hazard rate and mean residual life. At the end, in this paper, we present applications where POLOGD performs as a more effective model relative to POLOG in fitting a dataset.

7. PARAMETER ESTIMATION

In this section, we find the estimates of parameters of the POLOG distribution by using the maximum likelihood (ML) method.

The log-likelihood function of the random sample x_1, x_2, \dots, x_n from POLOGD is

$$\ln(L) = \left[\begin{array}{l} n \ln(1-p) + n \ln(\alpha) + n \ln(\beta) + n\alpha \ln(\lambda) + (\beta-1) \sum_{i=1}^n \ln(x_i) \\ -(\alpha+1) \sum_{i=1}^n \ln(\lambda + x_i^\beta) - 2 \sum_{i=1}^n \ln \left\{ 1 - p\lambda^\alpha (\lambda + x_i^\beta)^{-\alpha} \right\} \end{array} \right] \quad (12)$$

The ML estimates can be obtained from the following equations when equated to zero.

$$\begin{aligned} \frac{\partial \ln(L)}{\partial \alpha} &= \frac{n}{\alpha} + n \ln(\lambda) - \sum_{i=1}^n \ln(\lambda + x_i^\beta) \\ &\quad - 2 \sum_{i=1}^n \frac{p\lambda^\alpha (\lambda + x_i^\beta)^{-\alpha} \ln(\lambda + x_i^\beta) - p\lambda^\alpha (\lambda + x_i^\beta)^{-\alpha} \ln \lambda}{1 - p\lambda^\alpha (\lambda + x_i^\beta)^{-\alpha}} \\ \frac{\partial \ln(L)}{\partial \beta} &= \frac{n}{\beta} + \sum_{i=1}^n \ln(x_i) - (\alpha+1) \sum_{i=1}^n \frac{x_i^\beta \ln x_i}{(\lambda + x_i^\beta)} - 2 \sum_{i=1}^n \frac{\alpha p \lambda^\alpha (\lambda + x_i^\beta)^{-\alpha-1} x_i^\beta \ln x_i}{1 - p\lambda^\alpha (\lambda + x_i^\beta)^{-\alpha}} \\ \frac{\partial \ln(L)}{\partial \lambda} &= \frac{n\alpha}{\lambda} - (\alpha+1) \sum_{i=1}^n (\lambda + x_i^\beta)^{-1} - 2 \sum_{i=1}^n \frac{\alpha p \lambda^\alpha (\lambda + x_i^\beta)^{-\alpha-1} - \alpha p \lambda^{\alpha-1} (\lambda + x_i^\beta)^{-\alpha}}{1 - p\lambda^\alpha (\lambda + x_i^\beta)^{-\alpha}} \\ \frac{\partial \ln(L)}{\partial p} &= -\frac{n}{1-p} + 2 \sum_{i=1}^n \frac{\lambda^\alpha (\lambda + x_i^\beta)^{-\alpha}}{1 - p\lambda^\alpha (\lambda + x_i^\beta)^{-\alpha}} \end{aligned}$$

We can solve this system of nonlinear equations by employing numerical iterative technique BFGS in optim command based on R-Language.

To assess the performance of the ML estimates of the distribution's parameters we conduct a simulation study by drawing 10,000 random samples of sizes $n=25,50,100$ from POLOG distributions with $\alpha=0.5,1,3$, $\beta=0.5,1,2$, $\lambda=0.5,1,2$ and $p=0.25,0.50,0.75$. Estimates of the parameters and their MSEs are provided in Table 6 of Appendix A5.

It can be seen that the ML estimates are close to the true values of the parameters, and their MSEs are also reasonably small. A larger sample size increases the efficiency of estimates.

7.1 Applications of POLOGD Model

We provide here the applications of the POLOGD to four real life datasets for which the models have been proposed in literature. For its comparative assessment, we consider these fitted and other relevant models. The models are for these datasets, POLOG (Rady et al., 2016), Burr-XII Geometric (B-XIIG) distribution (Korkmaz & Erisoglu, 2014), Transmuted Exponentiated generalized Weibull (TExG-W) distribution (Yousof et al., 2015), Gamma distribution (GD) (Bhaumik et al., 2009), Beta Exponentiated Lomax distribution (BELD) (Mead, 2016) and Generalized compound Rayleigh distribution

(GCRD) (Bekker et al., 2007). The criteria used for comparison are AIC, BIC, CAIC, HQIC. Additionally, we apply generally known powerful tests - Cramer Von Mises test (W) and Anderson Darling test (A) to provide the probability of acceptance of selected model.

The datasets (references indicated) that we use for our applications, are given in Appendix A6 for the convenience of readers.

- **Application 1** (Dataset I)
A random sample of 128 bladder cancer patients on remission times (months) was used by (Rady et al., 2016) for fitting the model POLOD.
- **Application 2** (Dataset II)
Bhaumik, Kapur and Gibbons (Bhaumik et al., 2009) fitted the Gamma distribution (GD) model to the Vinyl chloride ($\mu\text{g}/\text{L}$) dataset consist of 34 observations from clean up gradient groundwater monitoring wells.
- **Application 3** (Dataset III)
Mead (Mead, 2016) applied Beta Exponential Lomax distribution to dataset of 40 observations on the active repair times (hours) for an airborne communication transceiver.
- **Application 4** (Dataset IV)
Bekker, Roux and Mosteit (Bekker et al., 2007) used this data on survival times (years) of 36 gastric cancer patients (who received chemotherapy treatment) in recommending Generalized compound Rayleigh distribution (GCRD) model.

7.1.1 Comparative Performance of POLOGD Model:

The best fitted models were proposed by the authors for the above data sets in the papers referred above. When comparing the models the choice of a superior one is based on its minimum measures of goodness criteria. As for application of Cramer Von Mises test (W) and Anderson Darling test (A), a larger probability associated with the model favors it. We now fit POLOGD model to each data set for its performance.

Below in the tables we provide information on the parametric estimates of fitted models, log-likelihood and the measures of goodness of fit; the results on POLOGD model are highlighted.

Table 1
Parametric Estimates of Fitted Models and Goodness of Fit Measures
for Dataset I ($n = 128$)

Model	$\hat{\alpha}$	$\hat{\beta}$	$\hat{\lambda}$	\hat{p}	$\hat{\phi}$	-2LL	AIC	BIC	HQIC	CAIC	W	A
POLOGD	2.86	1.53	178	0.71	---	820	827	839	832	828	0.9982	0.9993
POLOD	0.33	3.47	48.2	---	---	866	872	881	876	873	0.9587	0.9684
B-XIIG	0.23	2.34	---	0.00	---	907	913	921	916	913	0.8782	0.9056
TEg-W	0.54	1.04	0.331	1.13	0.167	825	835	849	840	835	0.9665	0.9751

Table 2
Parametric Estimates of Fitted Models and Goodness of Fit Measures
for Dataset II ($n = 34$)

Model	$\hat{\alpha}$	$\hat{\beta}$	$\hat{\lambda}$	\hat{p}	$\hat{\phi}$	-2LL	AIC	BIC	HQIC	CAIC	W	A
POLOGD	0.51	0.9889	5.283	0.896	---	123	131	137	133	132	0.9751	0.9896
POLOD	4.39	0.7336	18.05	---	---	147	153	157	154	153	0.9363	0.9675
GD	0.19	232.60	---	---	---	183	187	190	188	188	0.8709	0.9277
TEG-W	4.95	0.5329	0	0.219	0.48	155	165	172	167	167	0.9034	0.9426

Table 3
Parametric Estimates of Fitted Models and Goodness of Fit Measures
for Dataset III ($n = 40$)

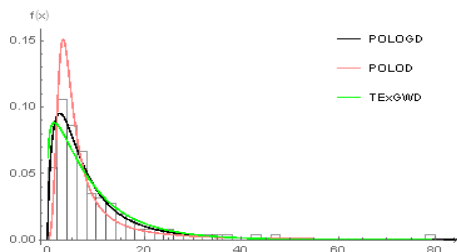
Model	$\hat{\alpha}$	$\hat{\beta}$	$\hat{\lambda}$	\hat{p}	$\hat{\phi}$	-2LL	AIC	BIC	HQIC	CAIC	W	A
POLOGD	153973	1	705760	0.2926	---	190	198	205	201	199	0.7536	0.7216
POLOD	24629	0.7288	44798	---	---	200	206	211	208	207	0.7023	0.6867
BLD	2599	0.0007	1191.0	179.5	---	313	321	328	324	322	0.6800	0.7025
BELD	0.0099	1160.1	0.0044	64.07	21.6	202	212	221	215	214	0.7189	0.6978

Table 4
Parametric Estimates of Fitted Models and Goodness of Fit Measures
for Dataset IV ($n = 36$)

Model	$\hat{\alpha}$	$\hat{\beta}$	$\hat{\lambda}$	\hat{p}	$\hat{\phi}$	-2LL	AIC	BIC	HQIC	CAIC	W	A
POLOGD	37.35	1.4915	630.89	0.9528	119	127	134	129	128	0.7302	0.7373	0.7216
POLOD	0.639	1.1268	0.4449	---	133	139	145	141	140	0.6925	0.7098	0.6867
BLD	46.14	317.95	1.7214	---	172	178	184	180	179	0.6844	0.7093	0.7025
BELD	0.242	0.2406	---	0.4201	286	292	297	294	292	0.6634	0.6874	0.6978

A comparison of models for each dataset based on information in the tables clearly indicates a general supremacy of our proposed POLOGD model.

Figure 6 (a, b, c and d) show the graphs of three estimated density curves which refer to POLOGD, POLOD and the third best of the remaining two models. The POLOGD density curves appear closer to the histograms described by the datasets.



**Figure 6(a): pdf Curves
Fitted to Dataset I**

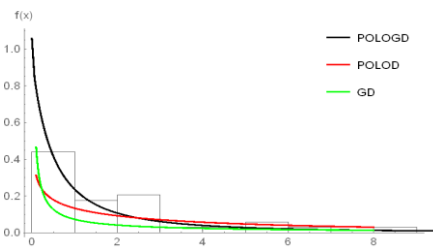


**Figure 6(b): pdf Curves
Fitted to Dataset II**

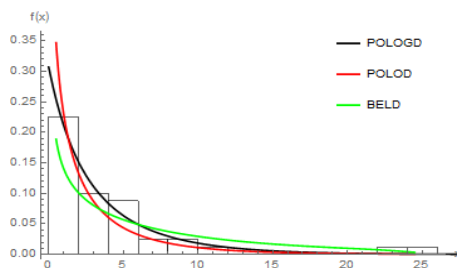


**Figure 6(c): pdf Curves
Fitted to Dataset III**

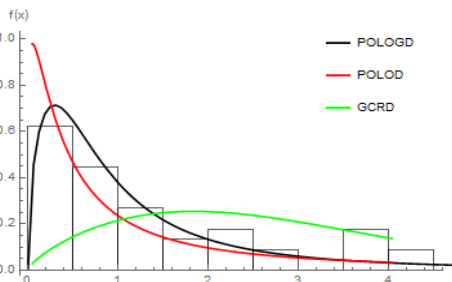


**Figure 6(d): pdf Curves
Fitted to Dataset IV**

8. CONCLUSION

Power Lomax Geometric distribution (POLOGD) proposed in this paper is the distribution of the minimum order statistic of a sample from Power Lomax distribution (POLOD) when the random sample size itself is geometrically distributed with an additional parameter p . So that POLOGD derived by compounding is a generalized form of POLOD and has four parameters. Since its family has heterogeneous characteristics, we classify it into three distinct versatile subfamilies. It is discovered that each subfamily has its unique theoretical and practical importance in fitting certain datasets. We estimate the parameters of this model by the maximum likelihood method, and provide applications of its three subfamilies to real life datasets for the description of which the best models have been suggested in literature. Its comparison is also made with other relevant models using goodness of fit measures. The preferable performance of the proposed model suggests that it can be a useful candidate for model fitting in various situations.

REFERENCES

1. Adamidis, K. and Loukas, S. (1998). A lifetime distribution with decreasing failure rate. *Stat. Probab. Lett.*, 39, 35-42.
2. Atkinson, A.B. and Harrison, A.J. (1979). The analysis of trends over time in the distribution of personal wealth in Britain. *Ann Insée.*, 33/34, 89-108. <https://doi.org/10.2307/20075322>.
3. Bekker, A., Roux, J.J.J. and Mosteit, P.J. (2007). A generalization of the compound Rayleigh distribution: using a Bayesian method on cancer survival times. *Commun. Stat. Theory Methods*, 29(7), 1419-1433. <https://doi.org/10.1080/03610920008832554>.

4. Bhaumik, D.K., Kapur, K. and Gibbons, R.D. (2009). Testing parameters of a Gamma distribution for small samples. *Technometric*, 51(3), 326-334. <https://doi.org/10.1198/tech.2009.07038>.
5. Bryson, M.C. (1974). Heavy-tailed distributions: properties and tests. *Technometrics*, 16(1), 61-68. <https://doi.org/10.1080/00401706.1974.10489150>.
6. Burr, I.W. (1942). Cumulative frequency functions. *Ann. Math. Stat.*, 13(2), 215-232.
7. Corbellini, A., Crosato, L., Ganugi, P. and Mazzoli, M. (2010). Fitting Pareto II distributions on firm size: Statistical methodology and economic puzzles. *Adv. Data Anal.*, 321-328, Springer.
8. Cordeiro, G.M., Ortega, E.M.M. and Popović, B.V. (2015). The Gamma-Lomax distribution. *J. Stat. Comput. Simul.*, 85(2), 305-319.
9. Ghitany, M.E., Al-Awadhi, F.A. and Alkhalfan, L. (2007). Marshall–Olkin extended Lomax distribution and its application to censored data. *Commun. Stat. Theory Methods*, 36(10), 1855-1866.
10. Glänzel, W. (1987). A characterization theorem based on truncated moments and its application to some distribution families. *Math. Stat. Probab. Theory*, 75-84, Springer.
11. Harris, C.M. (1968). The Pareto distribution as a queue service discipline. *Oper Res.*, 16(2), 307-313. <https://doi.org/10.1287/opre.16.2.307>.
12. Hassan, A.S. and Al-Ghamdi, A.S. (2009). Optimum step stress accelerated life testing for Lomax distribution. *J. Appl. Sci. Res.*, 5(12), 2153-2164.
13. Hassan, A.S. and Abd-Allah, M. (2017). Exponentiated Lomax Geometric distribution: properties and applications. *Pak. J. Stat. Oper. Res.*, 13(3), 545-566. <https://doi.org/10.18187/pjsor.v13i3.1437>.
14. Holland, O., Golaup, A. and Aghvami, A.H. (2006). Traffic characteristics of aggregated module downloads for mobile terminal reconfiguration. *IEE Proc. Commun.*, 153(5), 683-690. <https://doi.org/10.1049/ip-com:20045155>.
15. Korkmaz, M.Ç. and Erisoglu, M. (2014). The Burr XII-Geometric distribution. *J. Selcuk. Univ. Nat. Appl. Sci.*, 3(4), 75-87.
16. Lemonte, A.J. and Cordeiro, G.M. (2013). An extended Lomax distribution. *Statistics(Ber)*, 47(4), 800-816. <https://doi.org/10.1080/02331888.2011.568119>.
17. Lomax, K.S. (1954). Business Failures: Another example of the analysis of failure data. *J. Am. Stat. Assoc.*, 49(268), 847-852. <https://doi.org/10.1080/01621459.1954.10501239>.
18. Mead, M.E. (2016). On five-parameter Lomax distribution: properties and applications. *Pak. J. Stat. Oper. Res.*, 12(1), 185-200. <https://doi.org/10.18187/pjsor.v11i4.1163>.
19. Okasha, H.M. and Al-Shomrani, A.A. (2019). Generalized linear Exponential distributions and its applications. *J. Comput. Appl. Math.*, 351, 198-211. <https://doi.org/10.18187/pjsor.v11i4.1163>.
20. Rady, E.H.A., Hassanein, W.A. and Elhaddad, T.A. (2016). The power Lomax distribution with an application to bladder cancer data. *SpringerPlus.*, 5(1), 1-22. <https://doi.org/10.1186/s40064-016-3464-y>.
21. Sen, S., Afify, A.Z., Al-Mofleh, H. and Ahsanullah, M. (2019). The Quasi Xgamma Geometric distribution with application in medicine. *Filomat.*, 33(16), 5291-5330.
22. Yousof, H.M., Afify, A.Z., Alizadeh, M., Butt, N.S., Hamedani, G.G. and Ali, M.M. (2015). The transmuted exponentiated generalized-G family of distributions. *Pak. J. Stat. Oper. Res.*, 11(4), 441-464. <https://doi.org/10.18187/pjsor.v11i4.1164>

APPENDIX A1:

Let $k = (1 - qp)/(1 - q)$ which is greater than 1 as $0 < p, q < 1$.

The three derivatives of x_q

$$\frac{dx_q}{d\alpha} = \lambda^{\beta-1} \frac{1}{\beta\alpha^2} (k^{\alpha-1} - 1)^{\beta-1} (1 - k^{\alpha-1})^{-1} k^{\alpha-1} \log(k) < 0.$$

$$\frac{dx_q}{dp} = -q\lambda^{\beta-1} ((1 - q)\alpha\beta)^{-1} (k^{\alpha-1} - 1)^{\frac{1}{\beta}-1} k^{\alpha-1-1} < 0.$$

For this assertion, we find the derivative

$$\frac{dx_q}{d\lambda} = \beta^{-1} \lambda^{\beta-1-1} \left[(k^{\alpha-1} - 1) \right]^{\beta-1} > 0.$$

$$\frac{dx_q}{d\beta} = -\beta^{-2} \left[\lambda \left\{ ((1 - qp)/(1 - q))^{\alpha-1} - 1 \right\} \right]^{\beta-1} \log \left[\lambda \left\{ ((1 - qp)/(1 - q))^{\alpha-1} - 1 \right\} \right]$$

which on increasing β remains positive or negative as $(1 - qp)/(1 - q)$ less than or more than $(1 + \lambda^{-1})^\alpha$ respectively.

APPENDIX A2:

Table 5
Descriptive Statistics of POLOGD

α	λ	p	β	Med	Mode	Mean	Sk	K	β	Med	Mode	Mean	Sk	K
			0.50	0.00018		0.0011	10.7	291.9	1.5	0.0567	0.0299	0.0687	1.38	5.73
		0.25	0.75	0.00322		0.0073	4.2	35.3	5	0.4228	0.4277	0.4206	0.10	2.84
			0.95	0.01077		0.0181	2.8	16.0	10	0.6502	0.6636	0.6433	0.49	3.35
			0.50	0.00010		0.0008	12.7	408.1	1.5	0.0456	0.0210	0.0582	1.62	6.79
	0.50	0.75	0.00208		0.0056	4.9	46.2		5	0.3961	0.3929	0.3970	0.04	2.82
		0.95	0.00764		0.0143	3.2	20.2		10	0.6293	0.6378	0.6244	0.37	3.19
			0.50	0.00003		0.0004	17.1	748.6	1.5	0.0306	0.0122	0.0428	2.10	9.51
	0.75	0.75	0.00093		0.0034	6.3	76.5		5	0.3512	0.3378	0.3569	0.27	2.95
		0.95	0.00406		0.0094	4.1	31.4		10	0.5926	0.5928	0.5911	0.17	3.05
			0.50	0.00073		0.0042	10.7	291.9	1.5	0.0900	0.0474	0.1090	1.38	5.73
	0.25	0.75	0.00810		0.0185	4.2	35.3		5	0.4856	0.4914	0.4832	0.10	2.84
		0.95	0.02233		0.0374	2.8	16.0		10	0.6969	0.7113	0.6895	0.49	3.35
			0.50	0.00038		0.0030	12.7	408.1	1.5	0.0724	0.0334	0.0923	1.62	6.79
21	1	0.50	0.75	0.00525		0.0141	4.9	46.2	5	0.4550	0.4514	0.4560	0.04	2.82
		0.95	0.01585		0.0297	3.2	20.2		10	0.6745	0.6836	0.6693	0.37	3.19
			0.50	0.00011		0.0017	17.1	748.6	1.5	0.0485	0.0193	0.0679	2.10	9.51
	0.75	0.75	0.00235		0.0087	6.3	76.5		5	0.4034	0.3881	0.4099	0.27	2.95
		0.95	0.00841		0.0194	4.1	31.4		10	0.6351	0.6353	0.6336	0.17	3.05
			0.50	0.00656		0.0378	10.7	291.9	1.5	0.1872	0.0987	0.2267	1.38	5.73
	0.25	0.75	0.03506		0.0800	4.2	35.3		5	0.6049	0.6121	0.6019	0.10	2.84
		0.95	0.07098		0.1091	2.8	16.0		10	0.7778	0.7939	0.7696	0.49	3.35
			0.50	0.00342		0.0273	12.7	408.1	1.5	0.1507	0.0694	0.1920	1.62	6.79
	3	0.50	0.75	0.02270		0.0612	4.9	46.2	5	0.5668	0.5623	0.5681	0.04	2.82
		0.95	0.05037		0.0858	3.2	20.2		10	0.7528	0.7630	0.7470	0.37	3.19
			0.50	0.00103		0.0151	17.1	748.6	1.5	0.1009	0.0402	0.1412	2.10	9.51
	0.75	0.75	0.01018		0.0375	6.3	76.5		5	0.5025	0.4834	0.5107	0.27	2.95
		0.95	0.02674		0.0552	4.1	31.4		10	0.7089	0.7091	0.7071	0.17	3.05
21				0.00038		0.0030	12.7	408.1		0.2691	0.2439	0.2803	0.51	3.12
25	1	0.5	0.5	0.00027		0.0021	11.8	336.0	3	0.2538	0.2303	0.2642	0.50	3.09
30				0.00019		0.0014	11.2	287.4		0.2387	0.2168	0.2483	0.49	3.06
40				0.00010		0.0008	10.4	240.1		0.2168	0.1971	0.2253	0.47	3.03
		0.25		0.0135		0.0215	2.57	13.83		0.0113		0.0179	2.51	13.16
	0.50			0.0097		0.0172	2.96	17.32		0.0082		0.0143	2.89	16.50
21	0.75	1		0.0053	Zero	0.0114	3.81	26.66	$\alpha = 25$	0.0045	Zero	0.0095	3.73	25.43
	0.25			0.0270		0.0430	2.57	13.83		0.0226		0.0359	2.51	13.16
	1	0.50		0.0195		0.0344	2.96	17.32		0.0164		0.0287	2.89	16.50
		0.75		0.0107		0.0228	3.81	26.66		0.0090		0.0190	3.73	25.43

APPENDIX A3:

It can be shown that the function $g(x) = cx^{c-1}/(a+x^c)$ with $a, x > 0$ decreases when x increases under the condition $0 < c \leq 1$. Otherwise, for $c > 1$, it describes a downward bathtub curve.

APPENDIX A4:

Lemma 1: Let $\psi(\alpha) = \alpha(1 - pc^\alpha)^{-1}$, where c, p are fixed numbers such that $0 < c < 1, \alpha > 0$ and $p \in (0, 1)$. Then $\psi(\alpha)$ is an increasing function of α .
The proof follows from the simple application of calculus.

APPENDIX A5:

Table 6
ML Estimates for the POLOG Distribution Parameters with their MSE
(in bold form)

$\alpha = 3, \lambda = 2$													
β	n	$p = 0.25$				$p = 0.5$				$p = 0.75$			
		α	β	λ	p	α	β	λ	p	α	β	λ	p
0.5	25	3.014	0.535	2.192	0.291	2.963	0.498	2.062	0.432	2.986	0.476	2.026	0.698
		0.099	0.010	0.860	0.057	0.027	0.006	0.616	0.050	0.005	0.004	0.254	0.022
	50	3.007	0.524	2.114	0.294	2.963	0.490	2.035	0.455	2.993	0.474	1.988	0.712
		0.073	0.004	0.352	0.036	0.020	0.003	0.252	0.027	0.001	0.003	0.038	0.012
	100	3.015	0.521	2.077	0.298	2.979	0.488	1.998	0.461	2.995	0.482	2.015	0.734
		0.038	0.002	0.112	0.019	0.008	0.001	0.067	0.012	0.000	0.001	0.003	0.002
1	25	3.033	1.037	2.946	0.350	2.975	0.052	1.998	0.401	2.991	0.927	2.010	0.696
		0.073	0.025	7.207	0.106	0.009	0.015	0.606	0.090	0.003	0.013	0.117	0.023
	50	2.984	1.004	2.116	0.232	2.988	0.944	2.001	0.450	2.994	0.940	1.973	0.700
		0.019	0.013	1.373	0.027	0.005	0.009	0.140	0.023	0.001	0.008	0.027	0.021
	100	3.001	1.002	2.054	0.238	2.992	0.956	1.982	0.465	2.998	0.951	2.000	0.730
		0.019	0.006	0.379	0.016	0.001	0.005	0.007	0.008	0.000	0.006	0.003	0.003
2	25	2.977	1.882	2.028	0.193	2.983	1.859	1.995	0.437	2.990	1.863	2.016	0.693
		0.017	0.057	0.510	0.073	0.004	0.053	0.110	0.063	0.002	0.052	0.053	0.031
	50	2.980	1.901	1.983	0.180	2.992	1.887	1.986	0.476	2.992	1.888	1.998	0.711
		0.012	0.030	0.046	0.067	0.002	0.030	0.005	0.013	0.001	0.032	0.011	0.010
	100	2.989	1.918	1.973	0.209	3.002	1.906	2.047	0.504	2.997	1.914	1.999	0.732
		0.006	0.020	0.012	0.049	0.000	0.022	0.006	0.005	0.000	0.020	0.002	0.004

$\beta = 2, p = 0.5$													
β	n	$\lambda = 0.5$				$\lambda = 1$				$\lambda = 2$			
		α	β	λ	p	α	β	λ	p	α	β	λ	p
0.5	25	0.487	2.348	0.541	0.546	0.466	2.407	1.048	0.538	0.445	2.488	2.047	0.516
		0.022	0.311	0.119	0.018	0.017	0.417	0.091	0.020	0.018	0.645	0.037	0.022
	50	0.493	2.240	0.506	0.529	0.480	2.267	1.014	0.525	0.461	2.321	2.031	0.517
		0.012	0.129	0.020	0.009	0.010	0.155	0.003	0.010	0.011	0.234	0.011	0.010
	100	0.485	2.149	0.500	0.524	0.483	2.165	1.013	0.521	0.473	2.189	2.021	0.518
		0.004	0.052	0.002	0.006	0.004	0.065	0.001	0.005	0.005	0.088	0.005	0.006
1	25	1.068	2.142	0.584	0.494	1.033	2.246	1.386	0.532	0.993	2.329	2.325	0.499
		0.136	0.134	0.539	0.035	0.093	0.200	1.850	0.050	0.085	0.272	1.624	0.051
	50	1.045	2.088	0.570	0.504	1.028	2.157	1.185	0.529	0.980	2.218	2.113	0.521
		0.066	0.062	0.203	0.025	0.040	0.074	0.809	0.020	0.031	0.116	0.329	0.017
	100	1.034	2.070	0.552	0.520	1.014	2.126	1.091	0.522	0.989	2.158	2.032	0.509
		0.023	0.027	0.108	0.011	0.010	0.037	0.206	0.010	0.010	0.053	0.046	0.007
3	25	3.002	1.868	0.530	0.482	2.997	1.855	1.033	0.460	2.983	1.859	1.995	0.437
		0.002	0.045	0.022	0.009	0.002	0.051	0.050	0.028	0.004	0.053	0.110	0.063
	50	3.006	1.903	0.526	0.486	3.004	1.886	1.025	0.488	2.992	1.887	1.986	0.476
		0.001	0.024	0.004	0.003	0.001	0.033	0.002	0.006	0.002	0.030	0.005	0.013
	100	3.008	1.936	0.506	0.496	3.007	1.925	1.015	0.490	2.995	1.912	2.007	0.484
		0.000	0.012	0.002	0.001	0.000	0.016	0.001	0.002	0.000	0.022	0.001	0.003

APPENDIX A6:

Data I: Remission times (months) of bladder cancer patients

0.08, 2.09, 3.48, 4.87, 6.94, 8.66, 13.11, 23.63, 0.20, 2.23, 3.52, 4.98, 6.97, 9.02, 13.29, 0.40, 2.26, 3.57, 5.06, 7.09, 9.22, 13.80, 25.74, 0.50, 2.46, 3.64, 5.09, 7.26, 9.47, 14.24, 25.82, 0.51, 2.54, 3.70, 5.17, 7.28, 9.74, 14.76, 26.31, 0.81, 2.62, 3.82, 5.32, 7.32, 10.06, 14.77, 32.15, 2.64, 3.88, 5.32, 7.39, 10.34, 14.83, 34.26, 0.90, 2.69, 4.18, 5.34, 7.59, 10.66, 15.96, 36.66, 1.05, 2.69, 4.23, 5.41, 7.62, 10.75, 16.62, 43.01, 1.19, 2.75, 4.26, 5.41, 7.63, 17.12, 46.12, 1.26, 2.83, 4.33, 5.49, 7.66, 11.25, 17.14, 79.05, 1.35, 2.87, 5.62, 7.87, 11.64, 17.36, 1.40, 3.02, 4.34, 5.71, 7.93, 11.79, 18.10, 1.46, 4.40, 5.85, 8.26, 11.98, 19.13, 1.76, 3.25, 4.50, 6.25, 8.37, 12.02, 2.02, 3.31, 4.51, 6.54, 8.53, 12.03, 20.28, 2.02, 3.36, 6.76, 12.07, 21.73, 2.07, 3.36, 6.93, 8.65, 12.63, 22.69.

Dataset II: Vinyl chloride from clean up gradient ground-water monitoring wells in ($\mu\text{g/L}$)

5.1, 1.2, 1.3, 0.6, 0.5, 2.4, 0.5, 1.1, 8, 0.8, 0.4, 0.6, 0.9, 0.4, 2, 0.5, 5.3, 3.2, 2.7, 2.9, 2.5, 2.3, 1, 0.2, 0.1, 0.1, 1.8, 0.9, 2, 4, 6.8, 1.2, 0.4, 0.2.

Dataset III: Active repair times (hours) for an airborne communication transceiver

0.50, 0.60, 0.60, 0.70, 0.70, 0.70, 0.80, 0.80, 1.00, 1.00, 1.00, 1.00, 1.10, 1.30, 1.50, 1.50, 1.50, 1.50, 2.00, 2.00, 2.20, 2.50, 2.70, 3.00, 3.00, 3.30, 4.00, 4.00, 4.50, 4.70, 5.00, 5.40, 5.40, 7.00, 7.50, 8.80, 9.00, 10.20, 22.00, 24.50.

Dataset IV: Survival times (years) of gastric cancer patients

0.047, 0.115, 0.121, 0.132, 0.164, 0.197, 0.203, 0.260, 0.282, 0.296, 0.334, 0.395, 0.458, 0.466, 0.501, 0.507, 0.529, 0.534, 0.540, 0.641, 0.644, 0.696, 0.841, 0.863, 1.099, 1.219, 1.271, 1.326, 1.447, 1.485, 1.553, 1.581, 1.589, 2.178, 2.343, 2.416, 2.444, 2.825, 2.830, 3.578, 3.658, 3.743, 3.978, 4.003, 4.033.